Global and Planetary Change 123 (2014) 139–149

Contents lists available at ScienceDirect

Global and Planetary Change

journal homepage: www.elsevier.com/locate/gloplacha

Anomalous South Pacific lithosphere dynamics derived from new total sediment thickness estimates off the West Antarctic margin

Florian Wobbe [a,*], Ansa Lindeque [b], Karsten Gohl [a]

[a] Alfred Wegener Institute for Polar and Marine Research, Am Alten Hafen 26, 27568 Bremerhaven, Germany
[b] TGS Geophysical Company (UK) Limited, 1 The Crescent, Surbiton, Surrey, KT6 4BN, United Kingdom

ARTICLE INFO

Article history:
Received 18 January 2014
Received in revised form 22 September 2014
Accepted 25 September 2014
Available online 28 October 2014

Keywords:
Sediment isopach map
Sediment thickness grid
Sediment volume
Residual basement depth
Dynamic topography
Paleotopography

ABSTRACT

Paleotopographic models of the West Antarctic margin, which are essential for robust simulations of paleoclimate scenarios, lack information on sediment thickness and geodynamic conditions, resulting in large uncertainties. A new total sediment thickness grid spanning the Ross Sea–Amundsen Sea–Bellingshausen Sea basins is presented and is based on all the available seismic reflection, borehole, and gravity modeling data offshore West Antarctica. This grid was combined with NGDC's global 5 arc minute grid of ocean sediment thickness (Whittaker et al., 2013) and extends the NGDC grid further to the south. Sediment thickness along the West Antarctic margin tends to be 3–4 km larger than previously assumed. The sediment volume in the Bellingshausen, Amundsen, and Ross Sea basins amounts to 3.61, 3.58, and 2.78 million km^3, respectively. The residual basement topography of the South Pacific has been revised and the new data show an asymmetric trend over the Pacific–Antarctic Ridge. Values are anomalously high south of the spreading ridge and in the Ross Sea area, where the topography seems to be affected by persistent mantle processes. In contrast, the basement topography offshore Marie Byrd Land cannot be attributed to dynamic topography, but rather to crustal thickening due to intraplate volcanism. Present-day dynamic topography models disagree with the presented revised basement topography of the South Pacific, rendering paleotopographic reconstructions with such a limited dataset still fairly uncertain.

1. Introduction

The accurate reconstruction of paleotopography is the main prerequisite for robust simulations of paleoclimate scenarios. Current paleotopographic models contain large uncertainties due to absent or sparse sediment thickness data and constraints on geodynamic conditions. Since the Southern Ocean plays an important role in global climate processes, we assess the sedimentary and geodynamic conditions of the Southern Pacific to ascertain these essential factors for modern paleotopographic reconstructions.

We present an improved sediment thickness grid for the West Antarctic margin, which is now based on all the available seismic reflection, borehole, and gravity modeling data. This new grid spans the Antarctic Peninsula, Bellingshausen Sea, Amundsen Sea, and Ross Sea and links to Whittaker et al.'s (2013) data off Victoria Land. In the first part of this publication, we compare our results to previous work and discuss possible implications for paleotopography and paleoclimate reconstructions of Antarctica.

In the second part, we analyze and re-evaluate the Late Cretaceous to present lithosphere dynamics of the South Pacific after the final breakup of Gondwana. The rifted continental margins of New Zealand and West Antarctica experienced different tectonic histories: As New Zealand drifted away from Antarctica it was subjected to excess tectonic subsidence of 500–900 m, with a maximum during the interval 70–40 Myr (Spasojevic et al., 2010; Sutherland et al., 2010). The conjugate Marie Byrd Land margin, by contrast, was deformed by movement of the Bellingshausen plate relative to Antarctica (Wobbe et al., 2012), affected by intraplate volcanism (Kipf et al., 2013), and covered by large amounts of glacial sediments (e.g., Rebesco et al., 1997; Scheuer et al., 2006a). The West Antarctic margin and its adjacent seafloor is currently more than 1000 m shallower than the conjugate New Zealand margin. It has been suggested that mantle upwelling following the Gondwana subduction cessation could have caused this anomalously high topography (e.g., Storey et al., 1999; Sieminski et al., 2003; Winberry and Anandakrishnan, 2004; Finn et al., 2005; Spasojevic et al., 2010; Sutherland et al., 2010). In order to test this hypothesis with new data, we determined the sediment-corrected basement topography for the South Pacific and compared it to (i) an empirical sediment-corrected depth model from the North Pacific (Crosby et al., 2006), (ii) various dynamic topography models (e.g., Ricard et al., 1993; Steinberger, 2007; Conrad and Husson, 2009; Spasojevic and Gurnis, 2012; Flament et al., 2013), and (iii) a current mantle shear wave velocity model (Schaeffer and Lebedev, 2013). The differences

* Corresponding author.
E-mail address: fwobbe@awi.de (F. Wobbe).

http://dx.doi.org/10.1016/j.gloplacha.2014.09.006

between the dynamic topography models are discussed and the implications for reconstructing the South Pacific paleobathymetry and paleotopography are highlighted.

2. Sediment thickness grids of the West Antarctic margin

We derived new 5 km and 5 arc minute resolution sediment thickness grids from seismic reflection and refraction data, from gravity models, and from data of selected drill sites on the West Antarctic margin of the Pacific (Ross Sea–Amundsen Sea–Bellingshausen Sea–Antarctic Peninsula).

2.1. Sediment thickness calculation

Total sediment thickness estimates of the continental margin and the deep ocean floor are largely based on multichannel seismic reflection surveys (Fig. 1). We used the two-way travel times (TWT) between the seafloor and the acoustic basement reflections along seismic reflection transects available from the Antarctic Seismic Data Library System (SDLS, Wardell et al., 2007, Table A.1 in the supplement) and along recently acquired and processed seismic profiles (e.g., ANT-18/5a, ANT-23/4, and ANT-26/3: Scheuer et al., 2006a,b; Lindeque and Gohl, 2010; Uenzelmann-Neben and Gohl, 2012; Wobbe et al., 2012; Gohl et al., 2013b; Kalberg and Gohl, 2014).

The TWT values, $2T$ in s, were converted to depth, Z in km, using Carlson et al.'s (1986) empirical relation $Z = 3.03\ln(1 - 0.52T)$. This method has been applied to seismic data acquired along the Antarctic Peninsula in past work (Rebesco et al., 1997; Scheuer et al., 2006a,b). Carlson et al.'s (1986) TWT–depth relationship is calibrated for sediments up to 1.4 km thick (~1.4 s TWT) only and the sediment thickness is considerably overestimated for TWTs larger than 2.8 s. This affects <5% of the data points, mainly located on the continental rise–slope transition. Due to the lack of area-wide seismic velocity models or downhole velocity measurements at drilling sites, we have to assume the acoustic velocity of sediments thicker than 2.8 s TWT.

P-wave velocities of 5–6 km thick sediments on the continental rise in polar regions typically range from 1800 to 4000 m s^{-1} (e.g., West Greenland, Chian et al., 1995; Suckro et al., 2012) or even 4200 m s^{-1} (e.g., East Greenland, Voss and Jokat, 2007). On the Amundsen Sea continental rise, sediment layer interval velocities from a P-wave refraction model (Lindeque and Gohl, 2010; Kalberg and Gohl, 2014) and from stacking velocities (Gohl et al., 2007; Uenzelmann-Neben and Gohl, 2012; Gohl et al., 2013b) range from 1600 to 4200 m s^{-1}. We determined the best fitting average acoustic velocity of sediments thicker than 2.8 s TWT to be 2818 m s^{-1} and converted all TWT values greater than 2.8 s to depth using this velocity.

The seismic data coverage of the Amundsen Sea Embayment shelf (Gohl et al., 2013b) is better than what the profiles used for this publication imply (Fig. 1). However, only few seismic lines reveal the top of basement, and those which do not were excluded. The limit of the sedimentary cover approaching the inner shelf is well documented (e.g., Gohl et al., 2013a,b, dotted line in Fig. 1).

2.2. Data merging and gridding

In order to extend data coverage of the mapped basement horizons from multichannel seismic data (Fig. 1) to the Ross Sea region, we incorporated total sediment thickness above the acoustic basement from Cooper et al. (1991). Wilson and Luyendyk (2009), whose data we included as well, estimated sediment thickness under the Ross Ice Shelf by extrapolating thickness trends in the Ross Sea from gravity anomalies. Four Deep Sea Drilling Project (DSDP) boreholes in the area of interest reach the basement. Their borehole depth measurements complement the sediment thickness data from the Ross Sea (sites 270 and 274, Hayes et al., 1975) and fill in the gaps of the most distal areas along the Antarctic Peninsula (sites 322 and 323, Hollister et al.,

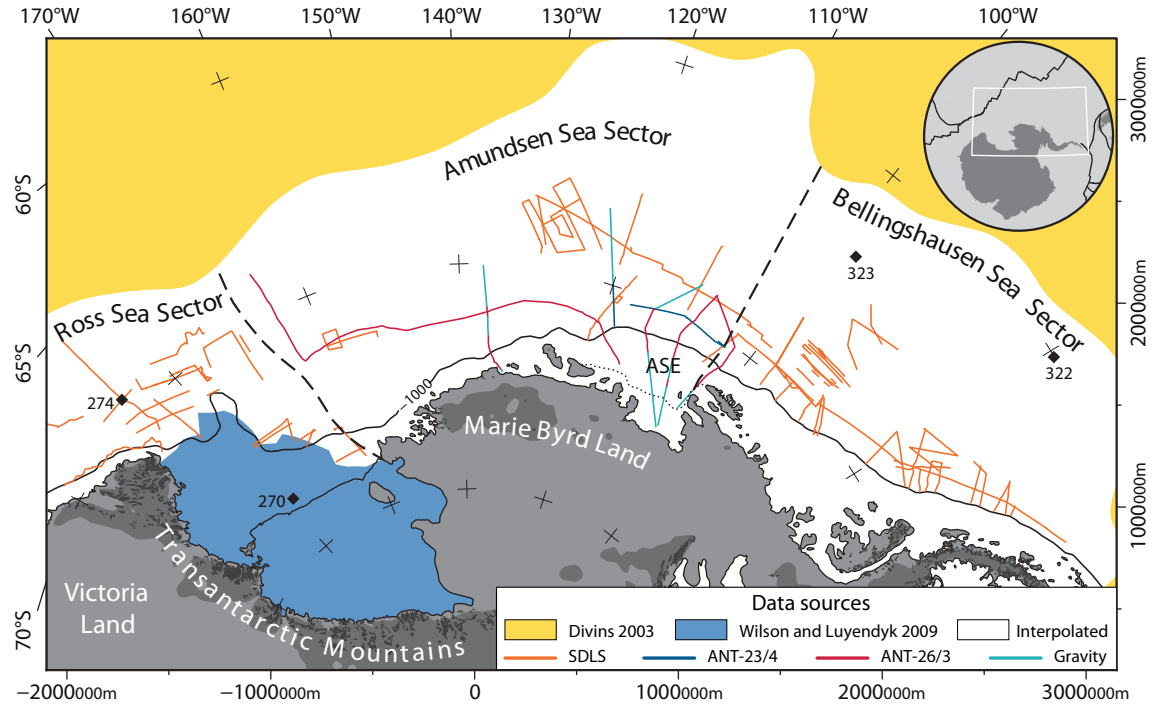

Fig. 1. Data sources used for compiling total sediment thickness and estimating sediment volumes. Areas based on gridded external data sources filled with solid colors (Divins, 2003; Wilson and Luyendyk, 2009). Data collected on transects are mostly multichannel seismic-reflection data available from the Antarctic Seismic Data Library System (SDLS, Wardell et al., 2007) and recent publications (ANT-23/4 and ANT-26/3: Scheuer et al., 2006a; Lindeque and Gohl, 2010; Uenzelmann-Neben and Gohl, 2012; Wobbe et al., 2012; Gohl et al., 2013b; Kalberg and Gohl, 2014). Some sediment thickness estimates in the Amundsen Sea sector are based on 2D gravity models (Wobbe et al., 2012). Dotted line outlines limit of sedimentary cover on inner Amundsen Sea Embayment (ASE) shelf (Gohl et al., 2013b). Polar stereographic projection with central meridian of 138°W and latitude of true scale at 71°S referenced to WGS84.

1976). Data from other DSDP, Ocean Drilling Project (ODP), and Antarctic Drilling (ANDRILL) drill sites along the West Antarctic margin were discarded because these boreholes do not yield the basement. Some sediment thickness estimates in the Amundsen Sea sector are based on a P-wave refraction model (Lindeque and Gohl, 2010; Kalberg and Gohl, 2014) and two-dimensional gravity models from Wobbe et al. (2012). The latter provide sediment thickness estimates along the axial extensions of adjacent seismic lines (light blue lines in Fig. 1). The limit of the sedimentary cover on the Amundsen Sea Embayment shelf was extrapolated east onto the Bellingshausen Sea shelf guided by gravity anomalies. We allocated values from the original ocean sediment thickness grid of the National Geophysical Data Center (NGDC, Divins, 2003) to areas further north and distant from the constrained data sources. These areas are roughly defined by the 100 m sediment isopach in the NGDC sediment thickness grid.

The compiled total sediment thickness point-based data (cf. Fig. A.1 in the supplement) were pruned by calculating 10 by 10 km block medians to remove short wavelengths and to avoid spatial aliasing during gridding. To fill the gaps between the points (white area in Fig. 1), the dataset was gridded using Smith and Wessel's (1990) continuous curvature splines algorithm with a tension factor of 0.2 to suppress local maxima and minima. Although data along the coastline were tapered to zero, we had to introduce about 150 further estimates of total sediment thickness to maintain a sensible appearance of the grid in areas remote from constrained sediment thickness. This is mostly the case, where the acoustic basement could not be identified on seismic profiles crossing the continental shelf. Our estimates are either plausible assumptions based on local geomorphology or inferred from the nearest constrained value.

Short range variations from the sediment thickness grid were removed by a second-order Butterworth low-pass filter with a cutoff wavelength of 100 km. We chose the Butterworth filter because it has no ripple in the passband at the expense of a relatively wide roll-off (Oppenheim and Schafer, 2009). The final grid was further resampled by bicubic interpolation to 5 km resolution. This new total sediment thickness grid is available in Antarctic Polar Stereographic Projection with a latitude of true scale at 71°S, referenced to WGS84 (Fig. 2).

The new regional Southern Pacific total sediment thickness grid was combined with the recently updated global sediment thickness grid of NGDC (Divins, 2003; Whittaker et al., 2013) to create an updated 5 by 5 minute global grid of ocean sediment thickness. The blending of the datasets was done by interpolating a 40 km buffer between the global and our smaller, regional grid, using continuous curvature splines with a tension factor of 0.2. The new total sediment thickness grids are available from PANGAEA (Wobbe et al., 2014).

2.3. Comparison to previous work and uncertainties

The presented total sediment thickness grid (Fig. 2) covers an area of more than 8 million km^2 and reveals major differences when compared to the sediment thickness compilation of Divins (2003). Divins' (2003) original NGDC global sediment thickness grid has recently been updated for the Australian–Antarctic region (Whittaker et al., 2013), as it became apparent that sediment thickness along the continental margins has been underestimated by more than 2000 m. The current NGDC grid, which excludes areas south of 70°S, largely underestimates sediment thickness off the Antarctic Peninsula and off Marie Byrd Land while slightly overestimating total sediment thickness around the De Gerlache Seamounts and the Marie Byrd Seamounts (cf. Figs. A.2 and A.3 in the supplement). Sediments in West Antarctic waters are approximately 4–4.8 km thick around the continental slope (approximately −1000 m contour in Fig. 2), which is about 3 km thicker than what Divins' (2003) NGDC compilation indicates. Sediments reach a maximum thickness of 6–8 km in glacial troughs on the Ross Sea shelf but taper off to less than 2 km further north. Total sediment thickness is estimated as larger than 4 km off the Antarctic Peninsula but less than 2–2.5 km off the coast of Marie Byrd Land and Victoria Land (west of DSDP site 274), and is maintained farther west (cf. Whittaker et al., 2013). Data from several proprietary seismic profiles (R/V Tangaroa, TAN0207 survey for the New Zealand UNCLOS program) off Chatham Rise indicate that Divins'

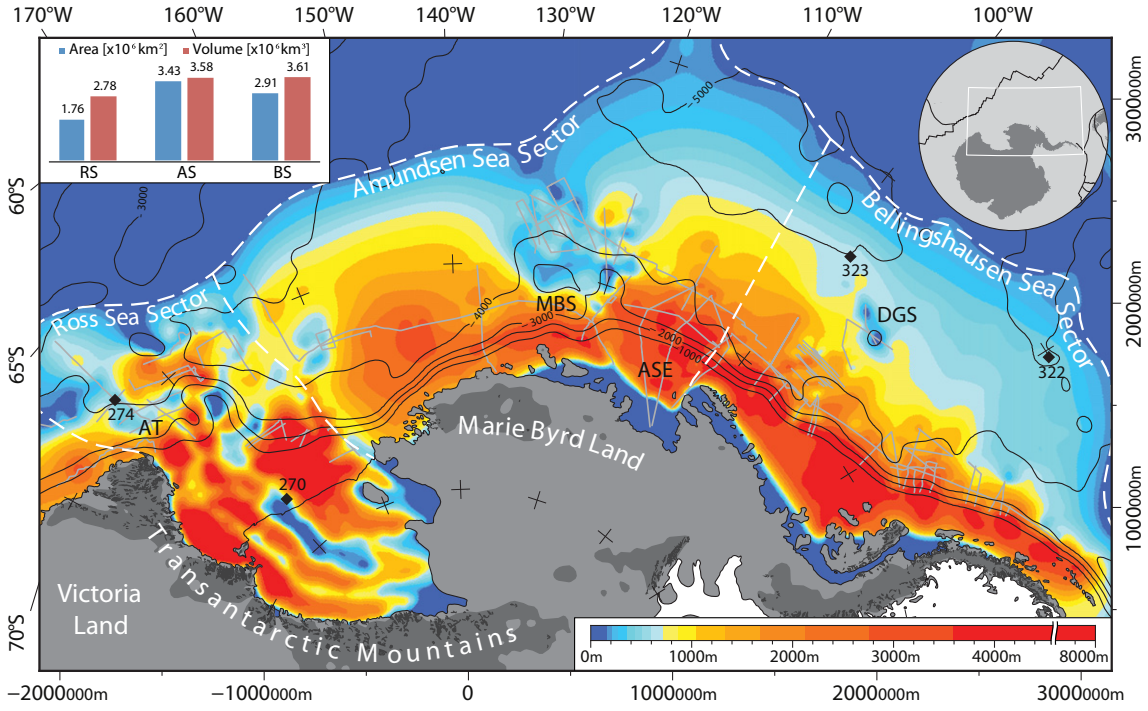

Fig. 2. The new total sediment thickness map of the Pacific margin of West Antarctica. Isopachs are color coded, contour lines indicate water depth in meter. White dashed lines delineate sediment catchment areas for the Ross Sea (RS), Amundsen Sea (AS) and Bellingshausen Sea (BS) basins. Compacted sediment volume estimates for these regions are illustrated in the top left corner. Black diamonds indicate locations of DSDP sites taken into account. Darker gray shading inland shows topography above 500 m. Rock outcrops from SCAR Antarctic Digital Database. AT — Adare Trough, DGS — De Gerlache Seamounts, MBS — Marie Byrd Seamounts. Polar stereographic projection with central meridian 138°W and true scale at 71°S.

(2003) sediment thickness estimates of West Antarctica's conjugate margin are accurate and do not compromise our residual basement depth calculation south of New Zealand in Section 3.

The mean West Antarctic sediment thickness (volume per deposition area ratio) varies slightly. It is largest in the Ross Sea and Bellingshausen Sea sectors (1.6 and 1.2 km), consistent with the very large flux associated with glacial sediment transport, and decreases to about 1.0 km in the Amundsen Sea sector. The total sediment volume amounts to 10 million cubic kilometers of which approximately 70% is equally distributed between the Amundsen and Bellingshausen Sea sectors (3.58 resp. 3.61×10^6 km^3), and the remaining 30% is spread across the Ross Sea sector (2.78×10^6 km^3).

Neglecting any margin parallel sediment transport, our calculations indicate that most of the terrigenous sediment influx from the West Antarctic originates from the smallest source area—the Antarctic Peninsula (15% of all area draining into the South Pacific). To illustrate this we determined the hypothetical minimum height of a sediment pile that would cover West Antarctica if all sediments were returned to their source areas by applying Wilson et al.'s (2012) estimates for in situ sediment density (1.95–2.1 g cm^3) and source rock density (2.6 g cm^3). DSDP and ODP boreholes around Antarctica yield a maximum pelagic fraction of 15%, which is not restored to the continent in this calculation. The terrigenous sediment source areas, draining into our three West Antarctic sectors, were determined from Zwally et al. (2012) present-day drainage system divides within the grounding line and west of the Transantarctic Mountains. Assuming these drainage system divides and their areas did not change with time, our calculations predict that sediments from the Ross Sea sector would pile up to a thickness of 2.9 km (or 640 m if source areas of East Antarctica are considered as well). Sediments from the Amundsen Sea sector would accumulate to a thickness of 3.8 km, and those from the Bellingshausen Sea sector would reach a height of 11 km. The very large value for the Bellingshausen drainage area can be explained by West Antarctica's high paleotopography (Wilson et al., 2012) which led to more erosion during the glacial. Earlier, subduction tectonics adjacent to the Antarctic Peninsula (e.g., Larter et al., 2002) may also have fostered an increased sediment influx into the basin.

Wilson and Luyendyk (2009) estimated a sediment volume of 2.0×10^6 km^3 above the oldest Ross Sea unconformity (RSU6, Oligocene and younger, e.g., Cooper et al., 1991). Our calculation takes into account a c. 30% larger Ross Sea deposition area and additional sediment thickness estimates along SDLS seismic reflection transects. Even though, the new sediment volume estimates above RSU6, 2.08×10^6 km^3, are not significantly larger, because the added distal deposition areas contain much less sediment than the ones in the central and western Ross Sea.

Although Scheuer et al.'s (2006a) sediment thickness grid of the Bellingshausen Sea and eastern Amundsen Sea shows east–west directed low frequency oscillation artifacts and occasionally large local minima and maxima, it compares reasonably well to our results in that the total sediment volume deviates by about 0.35×10^6 km^3 (cf. Figs. A.2 and A.3 in the supplement). This similarity can be attributed to the common database constraining the sediment thickness along seismic profiles, whereas the deviation is likely caused by a varied degree of data pruning and low-pass filtering.

The accuracy of the presented total sediment thickness grid varies proportionally to the distribution and abundance of seismic data offshore West Antarctica (Fig. 1). To a lesser degree, the sediment thickness data is affected by the TWT to depth conversion uncertainties rooted in the lack of seismic velocity models and drilling sites with key constraining downhole velocity data. The Ross Sea area is exceptionally well surveyed with a densely distributed seismic profile network and two basement yielding DSDP sites provide good calibration. The continental rise and slope within all sectors, except the westernmost and deeper Amundsen Sea are well mapped. In other places, where total sediment thickness is less constrained due to the absence of seismic reflection and borehole data, the thickness was interpolated over several hundred to thousand kilometers. Fortunately, most of these less constrained areas fall into the abyssal plains north of 70°S in the western Amundsen Sea sector, and north of 65°S in the eastern Amundsen Sea and Bellingshausen Sea sectors, where DSDP sites 322 and 323 hardly reported any sediment cover. Sediment thickness on the shelves of the Bellingshausen Sea and western Amundsen Sea could not be constrained by data but were based on observations from the central and eastern Amundsen Sea shelves. The largest uncertainties in the total sediment thickness grid are the limit of sedimentary cover and the sediment thickness on the inner Bellingshausen Sea.

3. Age of the oceanic lithosphere and basement depth

In Figs. 3 to 5 we present the derived set of digital grids that represent the South Pacific ocean floor ages, sediment-corrected basement depth, and oceanic residual basement depth. Collectively these provide an opportunity to study lithosphere dynamics of the West Antarctic margin. The residual basement depth (Fig. 5) is the difference between the sediment-unloaded basement depth (Fig. 4) and the predicted basement depth. The latter was derived from converting the crustal age (Fig. 3, Wobbe et al., 2012) to basement depth by using Crosby et al.'s (2006) North Pacific depth–age relationship, $d = -2821 - 315\sqrt{t}$.

We decided to apply Crosby et al.'s (2006) model for converting age to depth because it is based on sediment-corrected basement depths from the Pacific, and because it is unbiased by igneous crustal thickening. Therefore, it is considered suitable for detecting anomalies in the basement depth caused by, e.g., hotspot swells, plateaus, and seamounts. It should be noted however, that the differences between this chosen model and models proposed by other authors such as Stein and Stein (1992) GDH1 depth–age relationship are marginal (cf. profile 6 in Fig. 7), and in the context of the scale of this study considered negligible for studying large-scale basement depth anomalies (see Müller et al., 2008). In brief, the differences between GDH1 and Crosby et al.'s (2006) depth–age relationship range from −32 to 360 m for ages less than or equal to 90 Myr. The mean difference is 87 m and the median difference equals 55 m during this time interval. Both models are remarkably similar for ages younger than 80 Myr, which encompasses more than 96% of the area of interest (Fig. 3). Subsequently, GDH1 follows a shallower trend than Crosby et al.'s (2006) depth–age relationship.

Sediment loading was estimated from our total sediment thickness grid (Fig. 2), using the relationship between sediment thickness and isostatic correction from Sykes (1996). We calculated the sediment-unloaded basement depth by subtracting the isostatic effect using the water depths of the International Bathymetric Chart of the Southern Ocean (IBCSO, Arndt et al., 2013).

3.1. Residual basement depth anomalies

The residual basement depth of the South Pacific (Fig. 5) is largely positive, with a few exceptions along the Udintsev, Hazen and Tharp fracture zones (labeled in Fig. 3), southeast of the Campbell Plateau, and northwest of the Antarctic Peninsula. A positive residual basement depth anomaly indicates that the sediment-unloaded basement is shallower than expected based on Crosby et al.'s (2006) half-space cooling model. The magnitude of the residual basement depth anomaly and its irregular surface tend to correlate with hotspot trails, and with the size and abundance of seamounts. The sediment-unloaded basement is generally shallower in proximity to Antarctica. This is reflected in the values of the mean residual basement depth of the Antarctic and Pacific plate, being 485 and 204 m, respectively. The depth variation is best expressed by the root mean square, 699 and 394 m, respectively.

Fig. 6 illustrates the sediment-unloaded basement depth and the predicted basement depth on selected profiles that are parallel to flow lines crossing the Pacific–Antarctic Ridge. The profiles, which were selected carefully to avoid undulations near fracture zones, confirm that

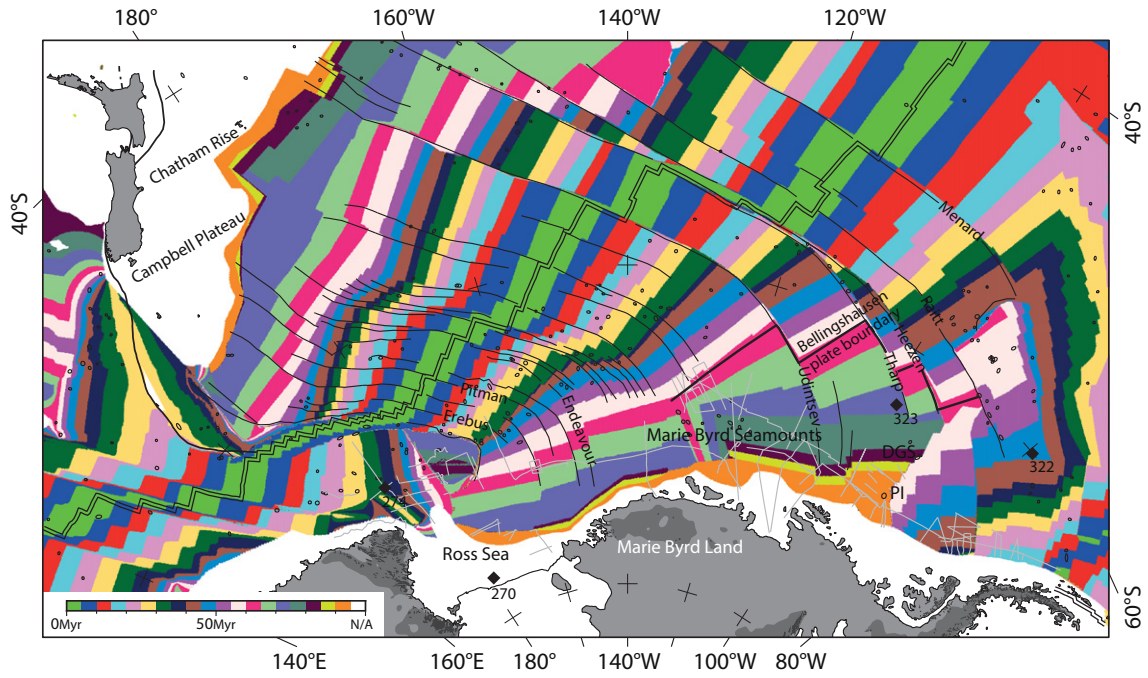

Fig. 3. Age of the oceanic lithosphere (Wobbe et al., 2012) overlain with locations of seamounts (black circles, Global Seamount Database, Kim and Wessel, 2011), fracture zones (black lines), and seismic and gravity profiles (light gray lines). Abbreviations same as Fig. 2 and PI — Peter I Island. Lambert conformal conic projection with central meridian 160°W and standard parallels 75°S and 69°S referenced to WGS84.

the sediment-corrected basement depth of the Antarctic plate is considerably higher than that of the Pacific plate. Due to the excessive sediment cover offshore West Antarctica, seafloor topography is more than 1000 m shallower compared to the conjugate New Zealand margin (Fig. 6). This is reflected by the isostatic correction for sediment thickness, which varies from 100 to 500 m south of the Campbell Plateau and Chatham Rise but then reaches 800–1500 m and, occasionally, more than 2000 m in the Ross Sea and Amundsen Sea. Despite the large difference in seafloor topography between the two conjugate margins, the sediment-unloaded basement depth, and hence the residual basement depth off Marie Byrd Land, usually differs by less than 250 m (Figs. 7 and A.4 in the supplement). Confined areas in the western Ross Sea, Marie Byrd Seamount area, and the Balleny Islands hotspot area south of the Pacific–Antarctic Ridge show residual basement depths exceeding 2000 m. Fig. 7 demonstrates that the residual basement depth usually oscillates between 0 and 500 m, and that a local

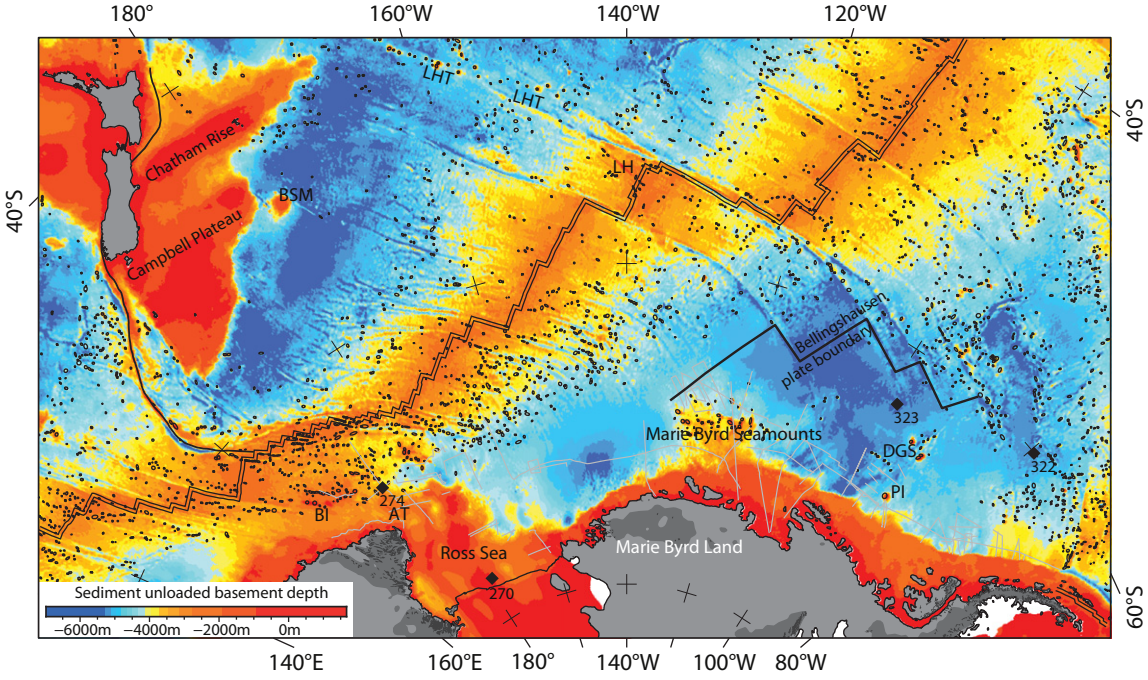

Fig. 4. Sediment-unloaded basement depth determined by applying the correction from Sykes (1996) using the sediment thickness from Fig. 2. Overlain with locations of seamounts (black circles, Global Seamount Database, Kim and Wessel, 2011). Abbreviations same as in previous figures and BI — Balleny Islands hotspot/Charcot Ridge, BSM — Bollons Seamount, LH — Louisville hotspot, LHT — Louisville hotspot trail. Lambert conformal conic projection with central meridian 160°W and standard parallels 75°S and 69°S.

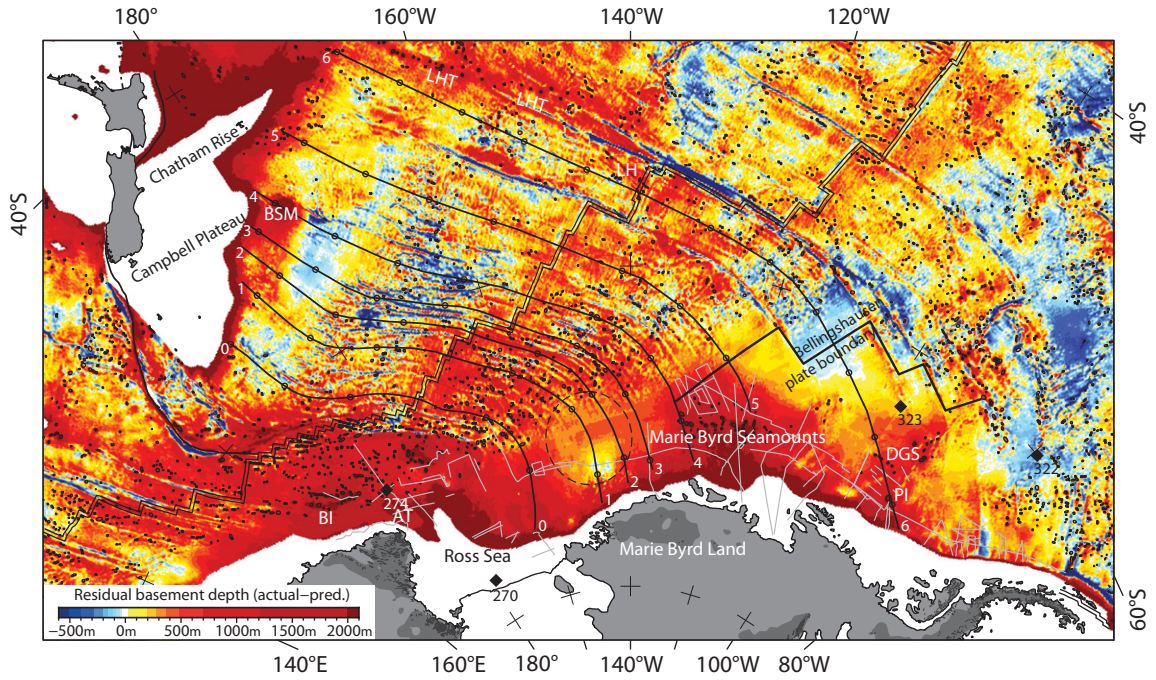

Fig. 5. Residual basement depth of the oceanic crust determined by calculating the difference between sediment-unloaded basement depth (Fig. 4) and predicted basement depth from applying Crosby et al.'s (2006) North Pacific depth–age relationship to the age distribution from Fig. 3. Profiles 0–6 along flow lines shown in Figs. 6, 7, and 10. Small circles along profiles placed 500 km apart. Dashed circle delineates Endeavour Anomaly. Abbreviations same as in previous figures. Lambert conformal conic projection with central meridian 160°W and standard parallels 75°S and 69°S.

maximum is located 200–700 km southeast from the Pacific–Antarctic Ridge in an area with a significantly higher seamount density (Global Seamount Database, Kim and Wessel, 2011 Fig. 5). Another distinctive feature within a circular area north of Marie Byrd Land is defined by an anomalously deep sediment-unloaded basement depth with values 500 m below the surrounding region. We name this the Endeavour Anomaly. The acoustic basement topography and sediment thickness at the Endeavour Anomaly are only constrained along a single west–east directed seismic profile across the Endeavour Fracture Zone (cf. Figs. 1 and 2). Further seismic data are not available in this region. The circular shape of the Endeavour anomaly is attributable to the interpolation algorithm used to grid the sediment thickness data, and its north–south expansion cannot be resolved.

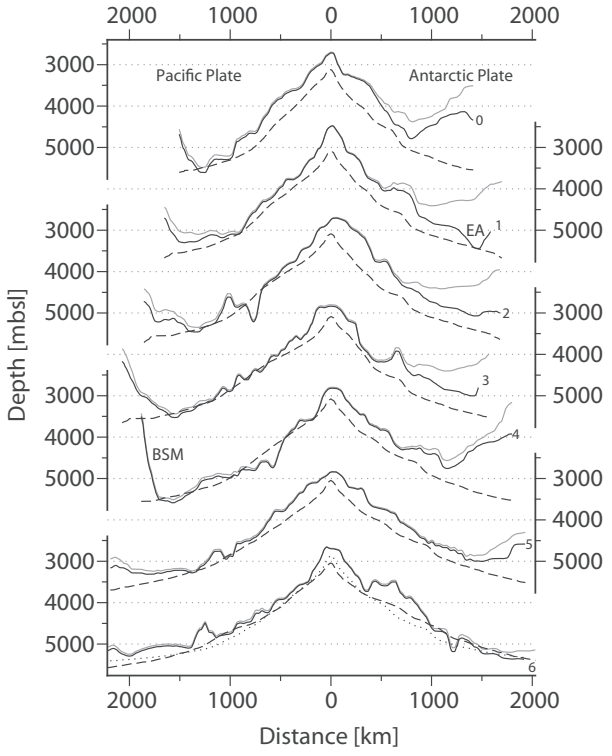

Fig. 6. IBCSO/GEBCO_08 bathymetry (gray line), sediment-unloaded basement depth from Fig. 4 (solid line), and predicted basement depth (dashed, Crosby et al., 2006) along profiles 0–6 across the Pacific–Antarctic Ridge (Fig. 5). Predicted basement depth from Stein and Stein's (1992) depth–age relationship (dotted line, profile 6, cf. Section 3). Abbreviations same as in previous figures and EA — Endeavour Anomaly.

3.2. Residual basement depth vs. seafloor roughness

Models explaining the morphology of mid-ocean ridge systems suggest that basement roughness depends on seafloor spreading rate and that an abrupt roughness intensification develops below a full spreading rate threshold of 60–70 mm Myr^{-1} (Small and Sandwell, 1989; Malinverno, 1991). This effect is readily visible in the roughness map in Fig. 8, where morphologically flat basement close to New Zealand and its conjugate margin off West Antarctica, formed along an initially fast spreading Pacific–Antarctic Ridge (>60 mm Myr^{-1}, Wobbe et al., 2012). Other parts of the ocean floor with large slope variability were formed less than 55 Myr ago when full-spreading velocities dropped below 60 mm Myr^{-1} (e.g., Larter et al., 2002; Eagles et al., 2004; Wobbe et al., 2012).

In the South Pacific, increased roughness is additionally caused by confined geological features including oceanic troughs, ridges, fracture zones, and seamounts. Cenozoic magmatism has been attributed to increased heat flow from the mantle (e.g., LeMasurier, 1990; Rocchi et al., 2002; Finn et al., 2005; Kipf et al., 2013). While seamounts such as the Balleny Islands, Marie Byrd Seamounts, De Gerlache Seamounts, and Peter I Island are limited morphological surface expressions of these magmatic centers, oceanic crust may respond to the underlying heat source with thermal uplift. Consequently, residual basement depth and seafloor roughness of the Antarctic plate often correlate (Figs. 5 and 8). However, the area with increased roughness between

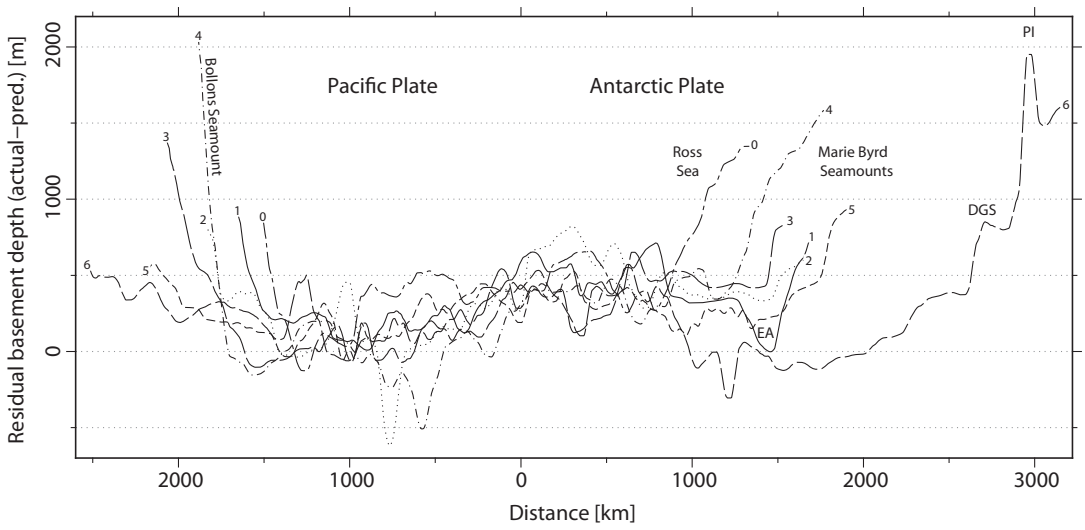

Fig. 7. Residual basement depth vs. distance from Pacific–Antarctic Ridge along profiles from Fig. 5. Abbreviations same as in previous figures.

Campbell Plateau and Pacific–Antarctic Ridge, for example, shows an opposing trend. Hence, seafloor roughness alone cannot be used to explain the residual basement depth distribution.

3.3. Residual basement depth vs. shear wave velocity

Schaeffer and Lebedev (2013) recently published a global tomographic shear wave velocity model of the upper mantle, which extends to a depth of 660 km. Fig. 9 displays the shear wave velocity anomaly of the uppermost mantle in four slices at different depths.

As expected, low shear wave velocities, which indicate increased heat flow in the mantle, coincide well with magmatic centers of Marie Byrd Land, Balleny Islands, and the Ross Sea area. In contrast, the Marie Byrd Seamounts, the De Gerlache Seamounts, and Peter I Island are underlain by mantle with anomalously high shear wave velocities that by implication may mean lower heat flow in the mantle. In these magmatic provinces off West Antarctica, the heat does not stem from the mantle directly below, as is the case in underplating, but may be provided by an upper mantle convective flow from warm mantle beneath the continental lithosphere of Marie Byrd Land (continental-insulation flow, Kipf et al., 2013, and references therein).

The distribution of seamounts that did not evolve from continental-insulation flow (e.g., Balleny Islands) matches the low shear wave velocity anomaly remarkably well. Similarly, the residual basement depth (Fig. 5) matches the shear wave velocity anomaly too. Noticeably, the shear wave velocity anomaly minimum below the mid-ocean ridges shifts asymmetrically in all depth slices. Particularly south of 60°S, the shear wave velocity anomaly is located 500 km south of the Pacific–Antarctic Ridge, where it also coincides with a local maximum of the residual basement depth (Figs. 7 and 10).

We chose Schaeffer and Lebedev's (2013) shear wave tomography as the most recently updated global mantle tomography model with

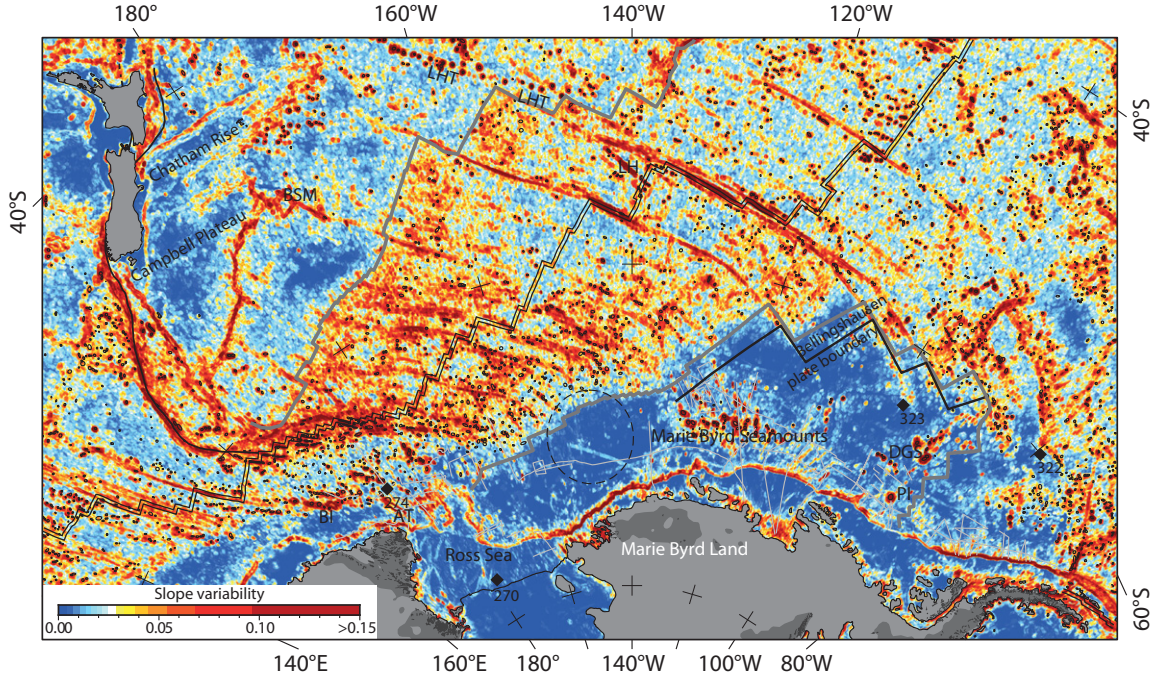

Fig. 8. Seafloor roughness computed by calculating the slope variability, $S_v = S_{max} - S_{min}$, over a 10′ × 10′ roving window from IBCSO/GEBCO_08 bathymetry. Thick gray lines are 55 Myr isochrons.

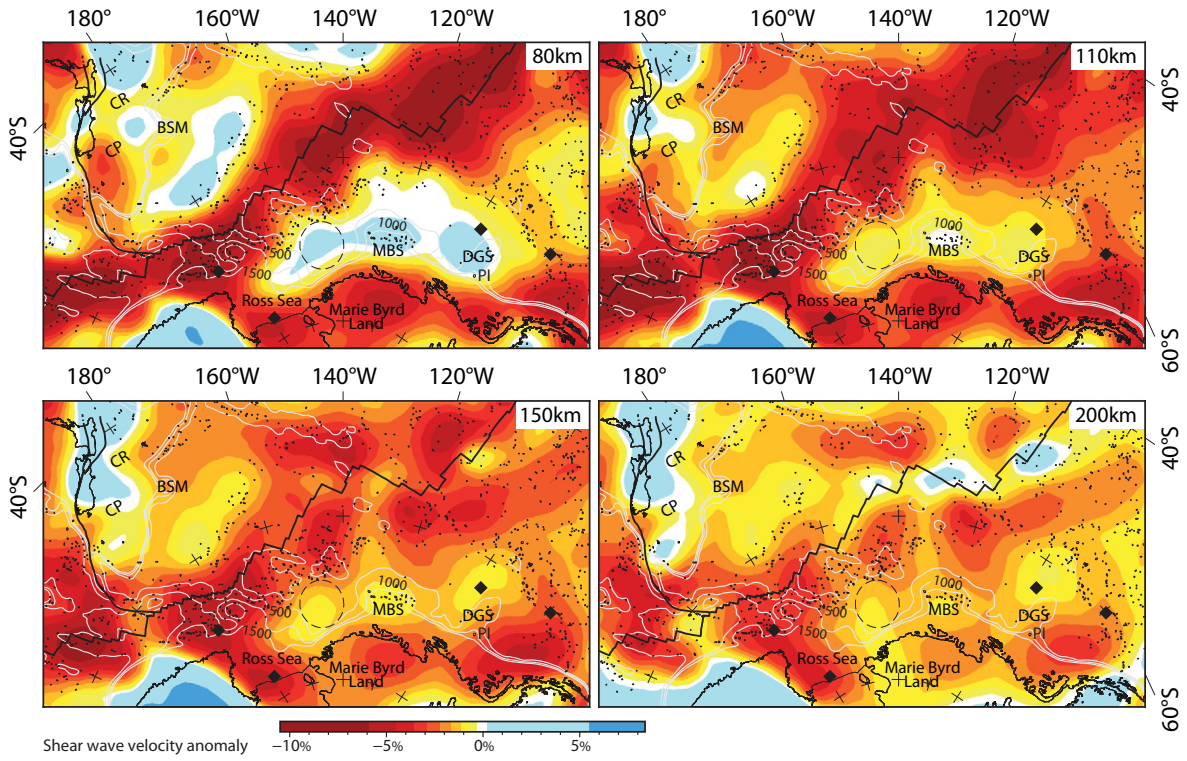

Fig. 9. Shear wave velocity anomalies (SL2013sv model, Schaeffer and Lebedev, 2013) of the upper mantle at 80, 110, 150, and 200 km depth with reference velocities of 4.38, 4.38, 4.39, and 4.45 km/s. Residual basement depth contours (500, 1000 and 1500 m) in gray.

major improvements on the resolution in oceanic regions and the Southern Hemisphere. However, the amplitude of the shear wave velocity anomaly in the study area decreases with depth and deviates less than 1% from zero at depths greater than 400 km. Distinct trends over the region or local extrema are absent. Well resolved shear wave velocity anomalies in this depth with an amplitude of less than 1% would require seismic velocity uncertainties better than 50 m s^{-1}.

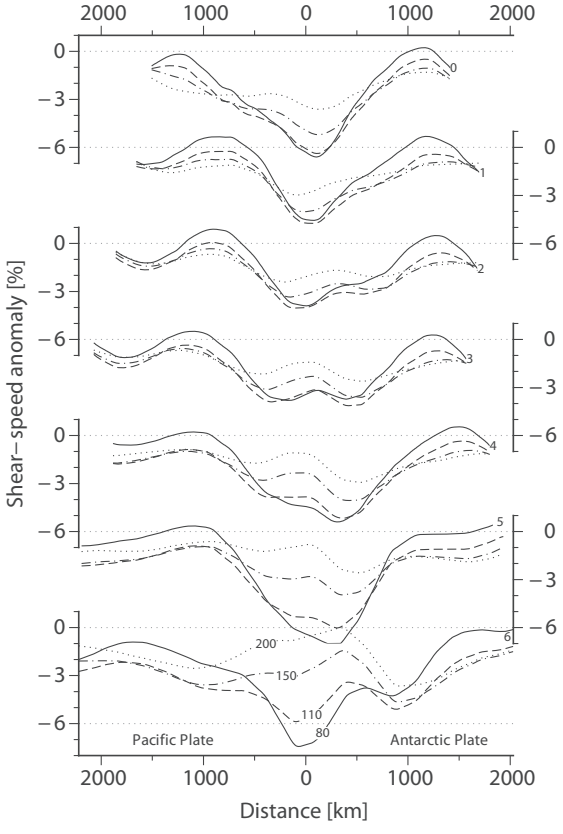

Fig. 10. Shear wave velocity anomalies of the upper mantle at 80, 110, 150, and 200 km depth vs. distance from Pacific–Antarctic Ridge along profiles 0–6 from Fig. 5.

4. Discussion

Improved paleoclimate and paleo-ice sheet models are subject to known limitations of current sediment volume approximations. With more robust sediment estimates, future reconstructions of paleotopography will improve our understanding of Antarctica's glaciation history. For instance, Wilson et al. (2013) estimated, based on the denudation history, that the total Antarctic ice volume since the Eocene–Oligocene transition was more than 1.4 times greater than previously assumed. This study and a recent work from Whittaker et al. (2013) both indicate that sediment thickness along the Antarctic margin has largely been underestimated. The landmass reduction of Antarctica due to erosion, therefore, has probably been larger than predicted (Wilson et al., 2012), and even larger ice sheet volumes may have covered Antarctica in the early times of glaciation. Of course, additional identifications of the volume and distribution of the pre-glacial to glacial components in the offshore sedimentary records are required in order to reconstruct the past topography for periods associated with large changes in climate proxies, such as the Eocene–Oligocene transition. However, the construction of pre-glacial to glacial sediment thickness grids is beyond the scope of this publication.

The previous section shows that there is a connection between residual basement depth and shear wave velocity on the one hand and magmatic processes on the other. Residual basement depth should also resemble the present-day dynamic topography. As opposed to isostatic topography resulting from density and thickness contrasts in the lithosphere, dynamic topography refers to the earth surface elevation effect due to mantle density inhomogeneities (e.g. Flament et al., 2013, and references therein). It develops over tens of millions of years and can exhibit several hundreds of meters in surface elevation

difference at long wavelengths. Dynamic topography models are derived from the present-day density structure of the mantle, subduction history, and plate-tectonic reconstructions. Uncertainties lie, for example, in the varying resolution of regional mantle convection models derived from global seismic tomography. As published dynamic topography models over the Southern Pacific suffer from large uncertainties, we compared our results with five different models (Ricard et al., 1993; Steinberger, 2007; Conrad and Husson, 2009; Spasojevic and Gurnis, 2012; Flament et al., 2013, Fig. A.5 in the supplement). These global studies of dynamic topography are limited to a lateral resolution of about 3000–5000 km. There are regional mismatches at scales below 10 000 km and even inverse correlations, especially in the Pacific realm (Flament et al., 2013). None of the five above mentioned dynamic topography models resolve local residual basement anomalies in the South Pacific. Although absolute amplitudes vary as much as 1500 m, all models propose a topographic high beneath the Pacific Plate, north of 60°S/150°W, which is in contrast with the residual basement depth (Fig. 5) and the shear wave anomaly (Fig. 9). Depending on the chosen model, dynamic topography beneath the Antarctic Plate and West Antarctica varies between −500 and 1000 m, and the magnitude beneath New Zealand is usually consistent with that beneath Marie Byrd Land.

Mantle upwelling following the Gondwana subduction cessation around 100 Myr (e.g. Laird and Bradshaw, 2004) has been suggested, but its extension beneath the West Antarctic margin remains unclear (e.g., Storey et al., 1999; Sieminski et al., 2003; Winberry and Anandakrishnan, 2004; Finn et al., 2005). However, basement depth, mantle shear wave velocity anomaly (Schaeffer and Lebedev, 2013), and Kipf et al.'s (2013) continental-insulation flow model show that upper mantle convective flow is solely confined to an area located beneath Marie Byrd Land and the Ross Sea. Spasojevic et al. (2010) and Sutherland et al. (2010) constructed models of Late Cretaceous to Cenozoic mantle flow, attributed to low density material above the Gondwana slab graveyard beneath Antarctica, to predict dynamic topography. Their models, which are based on present-day bathymetry, explain the high topography of the Ross Sea and Marie Byrd Land region as well as anomalous postrift Campbell Plateau subsidence. Our findings complement Sutherland et al.'s (2010) dynamic topography model, and our total sediment thickness estimates confine areas of anomalous basement elevation more precisely. For example, Sutherland et al. (2010) attributed excess topography (0.5–2.0 km) offshore Marie Byrd Land and in the Ross Sea region to dynamic topography. Our results confirm this for the Ross Sea as well as the Balleny Islands hotspot area. However, the residual basement depth off Marie Byrd Land does not exceed that south of Campbell Plateau by more than 250 m (Figs. 7 and A.4 in the supplement). East of the Ross Sea area, anomalously high basement topography is associated with magmatic processes driven by continental-insulation flow only (Marie Byrd Seamounts, De Gerlache Seamounts, Peter I Island, e.g., Kipf et al., 2013). Oceanic crust elsewhere in that region seems unaffected by mantle processes (e.g., Endeavour Anomaly). Sutherland et al.'s (2010) present day dynamic topography model coincides with our positive residual basement depth anomaly in the Ross Sea, but their proposed topography high beneath the Pacific Plate north of the Pacific–Antarctic Ridge lacks an equal counterpart anomaly in the residual basement depth.

A peculiar feature of the residual basement anomaly is its asymmetry over the Pacific–Antarctic Ridge, with a local maximum south of the spreading center, exactly where Campbell Plateau passed through—according to recent South Pacific plate motion models (e.g., Larter et al., 2002; Eagles et al., 2004; Wobbe et al., 2012)—during 70–40 Myr (cf. Fig. A.6 in the supplement). This time interval also marks the peak subsidence of the Campbell Plateau as it moved away from Antarctica to its present-day position (Sutherland et al., 2010). Although residual basement depth represents only a snapshot of dynamic topography, which occurs over tens of millions of years (Flament et al., 2013), the anomalous basement elevation south of the Pacific–Antarctic Ridge seems to be caused by processes persisting since the Cretaceous separation of New Zealand from Antarctica. It should be kept in mind, though, that until more robust dynamic topography models become available, predictions of the South Pacific paleotopography remain highly speculative.

5. Conclusions

Seismic data, recently acquired along the West Antarctic margin, suggests that Divins' (2003) minimum sediment thickness estimates along the West Antarctic margin are much too low. We present a new total sediment thickness grid spanning the Ross Sea–Amundsen Sea–Bellingshausen Sea basins based on available seismic reflection, borehole, and gravity modeling data in West Antarctica (Fig. 2). Our sediment thickness and volume estimates are consistent with previous analyses that indicate larger sediment amounts on Antarctica's margin than previously assumed (e.g., Rebesco et al., 1997; Scheuer et al., 2006a; Whittaker et al., 2013). We therefore extended Divins' (2003) original NGDC grid further south by merging our new data with data from Scheuer et al. (2006a), Wilson and Luyendyk (2009), and Whittaker et al. (2013) into an updated 5 by 5 minute global grid of total ocean sediment thickness. The sediment thickness estimation involved interpolation over areas without data constraints, but fortunately most of the less constrained areas fall into the abyssal plains where sediment cover is usually sparse. Due to a wider, better constrained dataset, the presented sediment volume estimates off West Antarctica are considered to be fairly accurate. The sediment volume is the largest in the Bellingshausen Sea basin, with 3.61 million km^3, although its sediment source area is the smallest (15% of all area draining into the South Pacific). Contrary, the Ross Sea basin, into which sediments are supplied from a much larger area (43%), contains just 2.78 million km^3 of sediment. The Amundsen Sea basin, into which 42% of the present-day West Antarctic landmass on the Pacific side drain, is estimated to contain 3.58 million km^3 of sediment.

We determined the sediment-corrected basement topography for the South Pacific from our total sediment thickness model (Fig. 4). In addition, we obtained the residual basement depth of the oceanic crust (Fig. 5) by subtracting the sediment-corrected basement depth from the theoretical basement depth, using a current South Pacific crustal age model (Wobbe et al., 2012) and Crosby et al.'s (2006) North Pacific depth–age relationship. The mean residual basement depths of the Antarctic and Pacific plate differ by about 300 m. The Antarctic Plate has a residual basement depth of nearly 500 m, but the excessive sediment cover offshore West Antarctica leads to seafloor depths in excess of 1000 m shallower than those of the conjugate New Zealand margin. No direct relationship between seafloor roughness (Fig. 8) and residual basement depth or overlying sediment accumulation has been observed. Ocean floor with large slope variability rather formed from 55 Myr ago until present, when full-spreading velocities dropped below 60 mm Myr^{-1}.

Dynamic topography models (e.g., Ricard et al., 1993; Steinberger, 2007; Conrad and Husson, 2009; Spasojevic and Gurnis, 2012; Flament et al., 2013) of the South Pacific are inconsistent with our local residual basement anomalies or even reversely correlate, and it remains unclear why. The pattern of residual basement depth, however, matches the distribution of seamounts and the shear wave velocity anomaly of the upper mantle (Fig. 9). Collectively these observations suggest that mantle dynamics play a role and that the resolution of dynamic topography models still lack the precision to pinpoint present-day small-scale residual basement anomalies. Our findings support Sutherland et al.'s (2010) model of Late Cretaceous to Cenozoic persistent mantle flow beneath West Antarctica following the Gondwana subduction cessation, but show that basement elevation, estimated from seafloor topography only, has been overestimated off Marie Byrd Land. We demonstrate through our analysis that the Marie Byrd Land margin is only affected by magmatic processes in the context of

continental-insulation flow (Kipf et al., 2013, e.g., Marie Byrd Seamounts, De Gerlache Seamounts, Peter I Island). This seems to be supported by the observation that oceanic crust farther away from these magmatic centers is elevated less than 250 m higher than oceanic crust from the conjugate New Zealand margin. The Ross Sea as well as the Balleny Islands hotspot area, and a region south of the Pacific–Antarctic Ridge, however, have been subject to mantle processes that lead to anomalously high basement elevations more than 1500 m higher as expected. A persistent basement high south of the ridge would explain the rapid subsidence of the Campbell Plateau during 70–40 Myr en route to its present day position. Until more accurate dynamic topography models, that can explain the present-day anomalous basement depth both at the Pacific–Antarctic Ridge and along the continental margins, become available, predictions of the South Pacific paleotopography remain speculative.

Acknowledgments

This project has been funded by the Earth System Sciences Research School (ESSReS), a graduate school of the Helmholtz Association of German Research Centres (HGF) at the Alfred Wegener Institute (AWI), and through the Priority Program 1158 'Antarctic Research' of the Deutsche Forschungsgemeinschaft under project number GO 724/10-1. We thank Doug Wilson and Carsten Scheuer, with whom we had helpful discussions, for sharing their results, and Nicolas Flament for the data exchange. Special thanks go to the New Zealand UNCLOS project for granting insight into seismic data off Chatham Rise. All of the figures in this publication were created using GMT (Generic Mapping Tools, Version 5, by Wessel et al., 2013). We thank Carmen Gaina and Joanne Whittaker for their constructive reviews.

Appendix A. Supplementary data

Supplementary data associated with this article can be found in the online version, at http://dx.doi.org/10.1016/j.gloplacha.2014.09.006. Gridded data sets are available from PANGAEA at http://dx.doi.org/10.1594/PANGAEA.835589.

References

Arndt, J.E., Schenke, H.W., Jakobsson, M., Nitsche, F.O., Buys, G., Goleby, B., Rebesco, M., Bohoyo, F., Hong, J., Black, J., Greku, R., Udintsev, G., Barrios, F., Reynoso-Peralta, W., Taisei, M., Wigley, R., 2013. The International Bathymetric Chart of the Southern Ocean (IBCSO) version 1.0 — a new bathymetric compilation covering circum-Antarctic waters. Geophys. Res. Lett. http://dx.doi.org/10.1002/grl.50413.

Carlson, R.L., Gangi, A.F., Snow, K.R., 1986. Empirical reflection travel time versus depth and velocity versus depth functions for the deep-sea sediment column. J. Geophys. Res. 91 (B8), 8249–8266. http://dx.doi.org/10.1029/JB091iB08p08249.

Chian, D., Louden, K.E., Reid, I., 1995. Crustal structure of the Labrador Sea conjugate margin and implications for the formation of nonvolcanic continental margins. J. Geophys. Res. Solid Earth 100 (B12), 24239–24253. http://dx.doi.org/10.1029/95JB02162.

Conrad, C.P., Husson, L., 2009. Influence of dynamic topography on sea level and its rate of change. Lithosphere 1 (2), 110–120. http://dx.doi.org/10.1130/L32.1.

Cooper, A.K., Davey, F.J., Hinz, K., 1991. Crustal extension and origin of sedimentary basins beneath the Ross Sea and Ross Ice Shelf. In: Thomson, M.R.A., Crame, J.A., Thomson, J.W. (Eds.), Geological Evolution of AntarcticaCambridge World and Regional Geology. Cambridge University Press, Cambridge. ISBN: 978-0521372664, pp. 285–291.

Crosby, A.G., McKenzie, D., Sclater, J.G., 2006. The relationship between depth, age and gravity in the oceans. Geophys. J. Int. 166 (2), 553–573. http://dx.doi.org/10.1111/j.1365-246X.2006.03015.x.

Divins, D.L., 2003. Total Sediment Thickness of the World's Oceans & Marginal Seas. NOAA National Geophysical Data Center, Boulder, CO Available from: http://www.ngdc.noaa.gov/mgg/sedthick/.

Eagles, G., Gohl, K., Larter, R., 2004. High-resolution animated tectonic reconstruction of the South Pacific and West Antarctic margin. Geochem. Geophys. Geosyst. 5, Q07002. http://dx.doi.org/10.1029/2003GC000657.

Finn, C.A., Müller, R.D., Panter, K.S., 2005. A Cenozoic diffuse alkaline magmatic province (DAMP) in the southwest Pacific without rift or plume origin. Geochem. Geophys. Geosyst. 6 (2). http://dx.doi.org/10.1029/2004GC000723.

Flament, N., Gurnis, M., Müller, R.D., 2013. A review of observations and models of dynamic topography. Lithosphere 5 (2), 189–210. http://dx.doi.org/10.1130/L245.1.

Gohl, K., Teterin, D., Eagles, G.G., Netzeband, G., Grobys, J.W.G., Parsiegla, N., Schlüter, P., Leinweber, V., Larter, R.D., Uenzelmann-Neben, G., Udintsev, G.B., 2007. Geophysical survey reveals tectonic structures in the Amundsen Sea Embayment, West Antarctica. In: Cooper, A.K., Raymond, C.R., the 10th ISAES Editorial Team (Eds.), Antarctica: A Keystone in a Changing World — Online Proceedings of the 10th International Symposium on Antarctic Earth SciencesUSGS Open-File Report 2007-1047, Short Research Paper 047. USGS. http://dx.doi.org/10.3133/of2007-1047.srp047.

Gohl, K., Denk, A., Eagles, G., Wobbe, F., 2013a. Deciphering tectonic phases of the Amundsen Sea Embayment shelf, West Antarctica, from a magnetic anomaly grid. Tectonophysics 585, 113–123. http://dx.doi.org/10.1016/j.tecto.2012.06.036.

Gohl, K., Uenzelmann-Neben, G., Larter, R.D., Hillenbrand, C.-D., Hochmuth, K., Kalberg, T., Weigelt, E., Davy, B., Kuhn, G., Nitsche, F.O., 2013b. Seismic stratigraphic record of the Amundsen Sea Embayment shelf from pre-glacial to recent times: evidence for a dynamic West Antarctic ice sheet. Mar. Geol. 344, 115–131. http://dx.doi.org/10.1016/j.margeo.2013.06.011.

Hayes, D.E., Frakes, L.A., Barrett, P.J., Burns, D.A., Chen, P.-H., Ford, A.B., Kaneps, A.G., Kemp, E.M., McCollum, D.W., Piper, D.J.W., Wall, R.E., Webb, P.N. (Eds.), 1975. Initial Reports of the Deep Sea Drilling Project vol. 28. U.S. Government Printing Office, Washington, D.C. http://dx.doi.org/10.2973/dsdp.proc.28.1975.

Hollister, C.D., Craddock, C., Bogdanov, Y.A., Edgar, N.T., Gieskes, J.M., Haq, B.U., Lawrence, J.R., Roegl, F., Schrader, H.-J., Tucholke, B.E., Vennum, W.R., Weaver, F.M., Zhivago, V.N., Worstell, P. (Eds.), 1976. Initial Reports of the Deep Sea Drilling Project vol. 35. U.S. Government Printing Office, Washington, D.C.. http://dx.doi.org/10.2973/dsdp.proc.35.1976.

Kalberg, T., Gohl, K., 2014. The crustal structure and tectonic development of the continental margin of the Amundsen Sea Embayment, West Antarctica: implications from geophysical data. Geophys. J. Int. 198 (1), 327–341. http://dx.doi.org/10.1093/gji/ggu118.

Kim, S.-S., Wessel, P., 2011. New global seamount census from altimetry-derived gravity data. Geophys. J. Int. 186 (2), 615–631. http://dx.doi.org/10.1111/j.1365-246X.2011.05076.x.

Kipf, A., Hauff, F., Werner, R., Gohl, K., van den Bogaard, P., Hoernle, K.A., Maicher, D., Klügel, A., 2013. Seamounts off the West Antarctic margin of the Pacific: a case of non-hotspot intraplate volcanism. Gondwana Res. http://dx.doi.org/10.1016/j.gr.2013.06.013.

Laird, M.G., Bradshaw, J.D., 2004. The break-up of a long-term relationship: the Cretaceous separation of New Zealand from Gondwana. Gondwana Res. 7 (1), 273–286. http://dx.doi.org/10.1016/S1342-937X(05)70325-7.

Larter, R.D., Cunningham, A.P., Barker, P.F., Gohl, K., Nitsche, F.O., 2002. Tectonic evolution of the Pacific margin of Antarctica 1. Late Cretaceous tectonic reconstructions. J. Geophys. Res. 107 (B12), 2345. http://dx.doi.org/10.1029/2000JB000052.

LeMasurier, W.E., 1990. Late Cenozoic volcanism on the Antarctic Plate: an overview. In: LeMasurier, W.E., Thomson, J.W., Baker, P., Kyle, P., Rowley, P., Smellie, J., Verwoerd, W. (Eds.), Volcanoes of the Antarctic Plate and Southern OceansAntarct. Res. Ser vol. 48. AGU, Washington, D.C.. ISBN: 978-0-87590-172-5, pp. 1–17. http://dx.doi.org/10.1029/AR048p0001.

Lindeque, A., Gohl, K., 2010. Western Antarctic palaeostratigraphy: implications for palaeobathymetry and palaeoclimate modelling. Poster presentation at IPY Oslo Science Conference, Oslo, 8–12 June 2010 Available from: http://elsevier.conference-services.net/resources/247/1976/pdf/Oslo2010_0377.pdf.

Malinverno, A., 1991. Inverse square-root dependence of mid-ocean-ridge flank roughness on spreading rate. Nature 352 (6330), 58–60. http://dx.doi.org/10.1038/352058a0.

Müller, R.D., Sdrolias, M., Gaina, C., Roest, W.R., 2008. Age, spreading rates, and spreading asymmetry of the world's ocean crust. Geochem. Geophys. Geosyst. 9, Q04006. http://dx.doi.org/10.1029/2007GC001743.

Oppenheim, A.V., Schafer, R.W., 2009. Discrete-time signal processing, Prentice Hall Signal Processing3 ed. Prentice Hall 978-0-13-198842-2.

Rebesco, M., Larter, R.D., Barker, P.F., Camerlenghi, A., Vanneste, L.E., 1997. The history of sedimentation on the continental rise west of the Antarctic Peninsula. In: Barker, P.F., Cooper, A.K. (Eds.), Geology and Seismic Stratigraphy of the Antarctic Margin, 2Antarct. Res. Ser vol. 71. AGU, Washington, D.C., pp. 29–49. http://dx.doi.org/10.1029/AR071p0029.

Ricard, Y., Richards, M., Lithgow-Bertelloni, C., Le Stunff, Y., 1993. A geodynamic model of mantle density heterogeneity. J. Geophys. Res. Solid Earth 98 (B12), 21895–21909. http://dx.doi.org/10.1029/93JB02216.

Rocchi, S., Armienti, P., D'Orazio, M., Tonarini, S., Wijbrans, J.R., Di Vincenzo, G., 2002. Cenozoic magmatism in the western Ross Embayment: role of mantle plume versus plate dynamics in the development of the West Antarctic Rift System. J. Geophys. Res. Solid Earth 107 (B9). http://dx.doi.org/10.1029/2001JB000515.

Schaeffer, A.J., Lebedev, S., 2013. Global shear-speed structure of the upper mantle and transition zone. Geophys. J. Int. http://dx.doi.org/10.1093/gji/ggt095.

Scheuer, C., Gohl, K., Eagles, G., 2006a. Gridded isopach maps from the South Pacific and their use in interpreting the sedimentation history of the West Antarctic continental margin. Geochem. Geophys. Geosyst. 7 (11), Q11015. http://dx.doi.org/10.1029/2006GC001315.

Scheuer, C., Gohl, K., Larter, R.D., Rebesco, M., Udintsev, G., 2006b. Variability in Cenozoic sedimentation along the continental rise of the Bellingshausen Sea, West Antarctica. Mar. Geol. 227 (3–4), 279–298. http://dx.doi.org/10.1016/j.margeo.2005.12.007.

Sieminski, A., Debayle, E., Lévêque, J.-J., 2003. Seismic evidence for deep low-velocity anomalies in the transition zone beneath West Antarctica. Earth Planet. Sci. Lett. 216 (4), 645–661. http://dx.doi.org/10.1016/S0012-821X(03)00518-1.

Small, C., Sandwell, D.T., 1989. An abrupt change in ridge axis gravity with spreading rate. J. Geophys. Res. Solid Earth 94 (B12), 17383–17392. http://dx.doi.org/10.1029/JB094iB12p17383.

Smith, W.H.F., Wessel, P., 1990. Gridding with continuous curvature splines in tension. Geophysics 55, 293–305.

Spasojevic, S., Gurnis, M., 2012. Sea level and vertical motion of continents from dynamic earth models since the Late Cretaceous. AAPG Bull. 96 (11), 2037–2064. http://dx.doi.org/10.1306/03261211121.

Spasojevic, S., Gurnis, M., Sutherland, R., 2010. Inferring mantle properties with an evolving dynamic model of the Antarctica–New Zealand region from the Late Cretaceous. J. Geophys. Res. Solid Earth 115 (B5). http://dx.doi.org/10.1029/2009JB006612.

Stein, C.A., Stein, S., 1992. A model for the global variation in oceanic depth and heat flow with lithospheric age. Nature 359 (6391), 123–129. http://dx.doi.org/10.1038/359123a0.

Steinberger, B., 2007. Effects of latent heat release at phase boundaries on flow in the Earth's mantle, phase boundary topography and dynamic topography at the Earth's surface. Phys. Earth Planet. Inter. 164 (1–2), 2–20. http://dx.doi.org/10.1016/j.pepi.2007.04.021.

Storey, B.C., Leat, P.T., Weaver, S.D., Pankhurst, R.J., Bradshaw, J.D., Kelley, S., 1999. Mantle plumes and Antarctica–New Zealand rifting: evidence from mid-Cretaceous mafic dykes. J. Geol. Soc. London 156 (4), 659–671. http://dx.doi.org/10.1144/gsjgs.156.4.0659.

Suckro, S.K., Gohl, K., Funck, T., Heyde, I., Ehrhardt, A., Schreckenberger, B., Gerlings, J., Damm, V., Jokat, W., 2012. The crustal structure of southern Baffin Bay: implications from a seismic refraction experiment. Geophys. J. Int. 190 (1), 37–58. http://dx.doi.org/10.1111/j.1365-246X.2012.05477.x.

Sutherland, R., Spasojevic, S., Gurnis, M., 2010. Mantle upwelling after Gondwana subduction death explains anomalous topography and subsidence histories of eastern New Zealand and West Antarctica. Geology 38 (2), 155–158. http://dx.doi.org/10.1130/G30613.1.

Sykes, T.J.S., 1996. A correction for sediment load upon the ocean floor: Uniform versus varying sediment density estimations—implications for isostatic correction. Mar. Geol. 133 (1–2), 35–49. http://dx.doi.org/10.1016/0025-3227(96)00016-3.

Uenzelmann-Neben, G., Gohl, K., 2012. Amundsen Sea sediment drifts: archives of modifications in oceanographic and climatic conditions. Mar. Geol. 299–302, 51–62. http://dx.doi.org/10.1016/j.margeo.2011.12.007.

Voss, M., Jokat, W., 2007. Continent–ocean transition and voluminous magmatic underplating derived from P-wave velocity modelling of the East Greenland continental margin. Geophys. J. Int. 170 (2), 580–604. http://dx.doi.org/10.1111/j.1365-246X.2007.03438.x.

Wardell, N., Childs, J.R., Cooper, A.K., 2007. Advances through collaboration: sharing seismic reflection data via the Antarctic Seismic Data Library System for Cooperative Research (SDLS). In: Cooper, A.K., Raymond, C.R., the 10th ISAES Editorial Team (Eds.), Antarctica: A Keystone in a Changing World — Online Proceedings of the 10th International Symposium on Antarctic Earth SciencesUSGS Open-File Report 2007-1047, Short Research Paper 001. USGS. http://dx.doi.org/10.3133/of2007-1047.srp001.

Wessel, P., Smith, W.H.F., Scharroo, R., Luis, J., Wobbe, F., 2013. Generic mapping tools: improved version released. EOS Trans. Am. Geophys. Union 94 (45), 409–410. http://dx.doi.org/10.1002/2013EO450001.

Whittaker, J., Goncharov, A., Williams, S., Müller, R.D., Leitchenkov, G., 2013. Global sediment thickness dataset updated for the Australian–Antarctic Southern Ocean. Geochem. Geophys. Geosyst. http://dx.doi.org/10.1002/ggge.20181.

Wilson, D.S., Luyendyk, B.P., 2009. West Antarctic paleotopography estimated at the Eocene–Oligocene climate transition. Geophys. Res. Lett. 36 (16), L16302. http://dx.doi.org/10.1029/2009GL039297.

Wilson, D.S., Jamieson, S.S.R., Barrett, P.J., Leitchenkov, G., Gohl, K., Larter, R.D., 2012. Antarctic topography at the Eocene–Oligocene boundary. Palaeogeogr. Palaeoclimatol. Palaeoecol. 24–34. http://dx.doi.org/10.1016/j.palaeo.2011.05.028 (Cenozoic Evolution of Antarctic Climates, Oceans and Ice Sheets).

Wilson, D.S., Pollard, D., DeConto, R.M., Jamieson, S.S., Luyendyk, B.P., 2013. Initiation of the West Antarctic ice sheet and estimates of total Antarctic ice volume in the earliest Oligocene. Geophys. Res. Lett. 40 (16), 4305–4309. http://dx.doi.org/10.1002/grl.50797.

Winberry, J.P., Anandakrishnan, S., 2004. Crustal structure of the West Antarctic rift system and Marie Byrd Land hotspot. Geology 32 (11), 977–980. http://dx.doi.org/10.1130/G20768.1.

Wobbe, F., Gohl, K., Chambord, A., Sutherland, R., 2012. Structure and breakup history of the rifted margin of West Antarctica in relation to Cretaceous separation from Zealandia and Bellingshausen plate motion. Geochem. Geophys. Geosyst. 13 (4), Q04W12. http://dx.doi.org/10.1029/2011GC003742.

Wobbe, F., Lindeque, A., Gohl, K., 2014. Total Sediment Thickness Grid of the Southern Pacific Ocean off West Antarctica, Data Repository. PANGAEA. http://dx.doi.org/10.1594/PANGAEA.835589.

Zwally, H.J., Giovinetto, M.B., Beckley, M.A., Saba, J.L., 2012. Antarctic and Greenland Drainage Systems, GSFC Cryospheric Sciences Laboratory, [online], Available from: http://icesat4.gsfc.nasa.gov/cryo_data/ant_grn_drainage_systems.php.